SUPPLEMENTARY MATERIAL

The structure of the Amyloid β-peptide high affinity Copper II binding site in Alzheimer's Disease

Victor A. Streltsov[*], Stephen J. Titmuss[*], V. Chandana Epa[*], Kevin J. Barnham[†‡§], Colin L. Masters[§†¶] and Joseph N. Varghese[*]

[*]CSIRO Molecular and Health Technologies, and Preventative Health Flagship, Parkville, VIC 3052, Australia and [†]Bio21 Molecular Science and Biotechnology Institute, [‡]Department of Pathology, [¶]Center for Neuroscience, The University of Melbourne, Parkville, Victoria, Australia, §Mental Health Research Institute of Victoria, Parkville, Victoria, Australia.

X-ray absorption data collection and radiation reduction. The X-ray absorption spectra of Cu^{1+} is characterized by a pre-edge feature in the 8980-8985 eV region of the XANES of the copper edge. This feature is not present for Cu^{2+}. The X-ray absorption spectra for the sample 2 (Aβ16-PB50: Aβ16Cu^{2+} in PB with 50% NaCl) is shown in Fig. 1S. The XANES region peak typical for Cu^{1+} at 8984 eV was increasing while the white line intensity was decreasing for each consecutive scan. These changes suggest that significant reduction (up to 7% in normalized absorption) of the copper occurred during the data collection for sample 2.

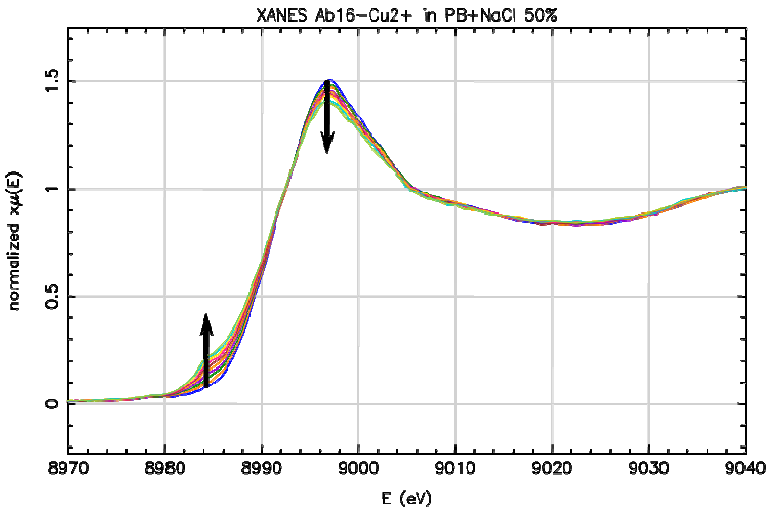

FIGURE 1S XANES region of the copper edge for 10 scans (40 min each scan).

Fig. 2S below presents the EXAFS regions of Aβ–Cu^{2+} spectra for all seven samples from Table 1. All spectra are generally similar except for sample 2 (Aβ16-PB50 – red line) which has altered peak profiles around k of 1.5, 4 and 6 $Å^{-1}$. This sample showed marked photo-reduction. The spectra also reflect the measurement uncertainty, ε_k, given in Table 1. The samples 5 (Aβ16-PBS), 6 (Aβ42M35V-PBS and particularly 7 (Aβ42M35(O)-PBS) are much noisier (higher ε_k) as expected for the lower concentration of the peptides. Overall features of Aβ42M35V (dark purple line) and Aβ42M35(O) (pink line) spectra are close to those of the short peptides spectra.

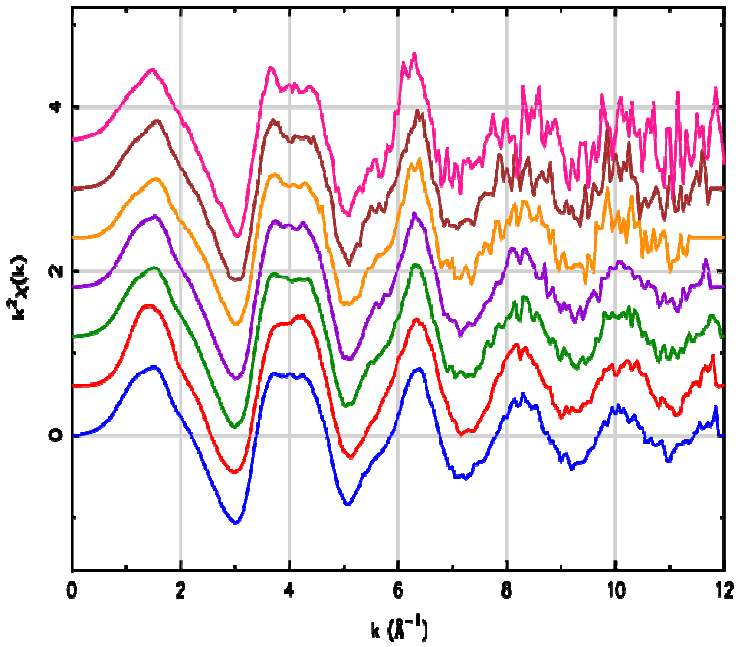

FIGURE 2S Superposition of Cu *K*-edge k^2-weighted EXAFS of all seven Aβ-Cu^{2+} samples as in Table 1 colored from bottom to top: Aβ16-PB - blue, Aβ16-PB50 - red, Aβ16-PB75 - green, Aβ16-PB100 - magenta, Aβ16-PBS - orange, Aβ42M35V-PBS – dark purple and Aβ42M35(O)-PBS - pink. The spectra are stacked with offset 0.5 units along the vertical axes.

The superimposed spectra for five samples (1: Aβ16-PB, 3: Aβ16-PB75, 4:Aβ16-PB100, 5:Aβ16-PBS, and 6:Aβ42-M35V) in the XANES region of 8960-9060 eV are shown in Figure 3S *A* and the enlarged XANES regions near spectral features at 8979, 8987, 8997, 9005, 9010 and 9045 eV marked as A, B, C, D, E and F, respectively, are shown in Figure 2S *B*, *C*, and *D* below. The noisy spectrum for sample 7: Aβ42-M35(Ox) is not included.

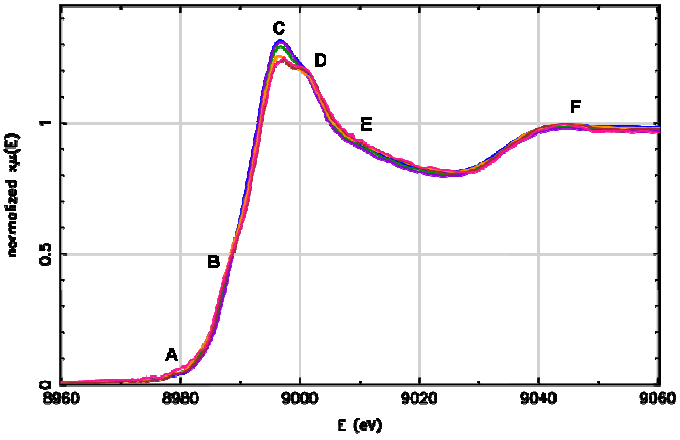

(*A*)

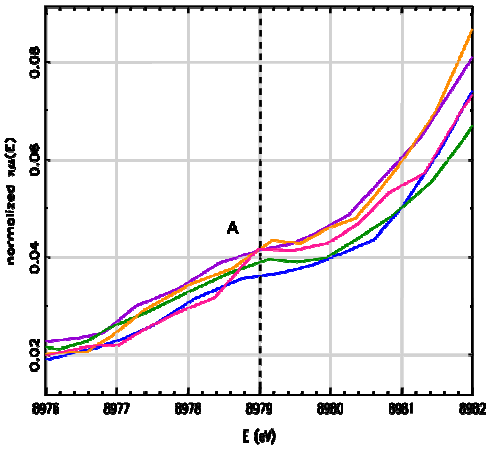

(*B*)

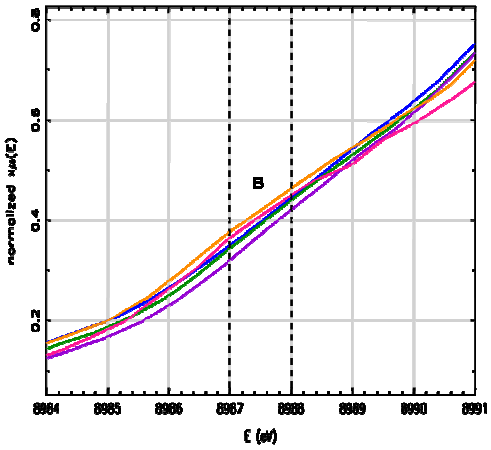

(*C*)

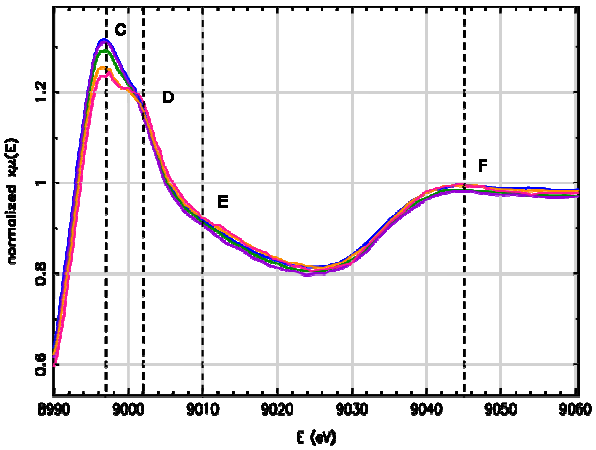

(*D*)

FIGURE 3S (*A*) The superimposed spectra for five samples (1:A*β*16-PB - blue , 3: A*β*16-PB75 – green , 4:A*β*16-PB100 - magenta, 5:A*β*16-PBS - orange, 6:A*β*42-M35V - pink). Spectral features at 8979, 8987, 8997, 9005, 9010 and 9045 eV are marked as A, B, C, D, E and F respectively; (*B*, *C* and *D*) the enlarged XANES regions around marked features.

X-ray absorption data analysis. The values of *R*-factor and χ^2 (reduced goodness-of-fit) were considered as parameters to measure goodness of the fit.

R-factor, $R = \frac{\sum_{i}^{N} f(r_i)^2}{\sum_{i}^{N} \chi_{data}(r_i)^2}$, and reduced goodness-of-fit, $\chi^2 = \frac{N_{ind}}{\varepsilon_k{}^2 N(N_{ind} - N_{\mathrm{var}})} \sum_{i=1}^{N} f(r_i)^2$,

were evaluated via the magnitude of the residual $f(r_i)^2 = f_{\mathrm{xafs}}(r_i)^2 + \Sigma(w\Delta_{\mathrm{restraint}}/\sigma_{\mathrm{restraint}})^2$ with $f_{\mathrm{xafs}}(r_i)$ defined as $f_{\mathrm{xafs}}(r_i) = \chi_{\mathrm{data}}(r_i) - \chi_{\mathrm{model}}(r_i)$, where $f(r_i)$, the minimized function which consists of the real and imaginary parts of the difference between the data $\chi_{\mathrm{data}}(r_i)$ and the model $\chi_{\mathrm{model}}(r_i)$ XAFS over the fit range r_i. The residual (penalty) function $\Delta_{\mathrm{restraint}}$ evaluates to 0 if the restraint expression is satisfied or is the difference between the two sides of the restraint expression; $\sigma_{\mathrm{restraint}}$ is the uncertainty value given for the restraint and derived here from the standard deviation of crystallographic structural parameters, and the weight *w* (the amplifier) determines the magnitude of the penalty. The final step of the refinements w conducted with *w*=1000. Further, ε_{k} is the measurement uncertainty in *k*-space; N_{var} is the number of variable in the fit; $N = 2(\Delta r)/\delta r$ is the number of data points in *r*-space with the grid spacing δr, and $N_{ind} = \frac{2(\Delta k + \Delta r)}{\pi}$ is the number of independent data points (1, 2) with data ranges $\Delta r = r_{\max} - r_{\min}$ and $\Delta k = k_{\max} - k_{\min}$ in *r*- and *k*- space, respectively.

Statistical F-test. In order to estimate if the difference between the two models is statistically significant or whether one model is significantly better than another, the statistical *F*-test was employed (3-5). Even though it is rigorously applicable to linear models, the *F*-test should represent a reliable approximation, especially, if the observed $F_{b,n-m}$ exceed not merely the selected percentage point, α, of the *F*-distribution, but several times (approximately four (3)) the selected percentage point:

$F_{b,n-m} = \frac{\chi_1^2 - \chi_2^2}{\chi_2^2} \frac{n - m_2}{b} >> F_{b,n-m,\alpha}$, where

χ^2_1 and χ^2_2 – reduced goodness-of-fit χ^2 for Model 1 and Model 2, respectively; $b = m_1 - m_2 =$

$(N_{ind} - N_{\mathrm{var1}}) - (N_{\mathrm{ind}} - N_{\mathrm{var2}})$ – degrees of freedom of *F*-distribution; $n - m_2 = (N_{\mathrm{ind}} - N_{\mathrm{var1}})$ – degrees of

freedom in χ^2_2.

Density Functional Theory investigation of starting models. The Density Functional Theory (DFT) method was applied on the proposed models of coordination around the Cu^{2+} ion in the Aβ-Cu^{2+} complexes. The DFT optimized geometries for Cu^{2+} bound to tyrosinate, three imidazoles and two water molecules (Model 2) is shown in Fig. 5S *A*.

Model 2 ("Tyr10") refinement. The best fits of the Model 2 to EXAFS multiple data sets is shown in Fig. 4S. The refined parameters are in Table 1S and the final geometry is shown in Fig. 5S *B*. The structures has a distorted six-coordinated copper ion with three imidazole nitrogen atoms (1.91-2.10 Å) and one tyrosinate (1.94-1.97 Å) oxygen atom in an approximately equatorial arrangement. The axial ligands are two water molecules placed asymmetrically (1.99-2.04 and 2.26-2.32 Å).

Table 1S. Best-fit EXAFS and DFT parameters of Model 2 for Aβ-Cu^{2+} complexes. (ΔE_o is the edge position relative to the photoelectron energy threshold E_o for samples: 1 - 8992.4, 3 - 8992.2, 4 - 8991.9, 5 - 8992.7 and 6 - 8992.4 eV); r_i and ϕ_i refer to the distances (in Å) and the polar angle (in degrees) for shell i; σ^2 Debye-Waller terms (in $Å^2$); N_{ind}, N_{var}, χ^2 and R are defined in the main text or in Supplementary Material; estimated standard deviation is given in parenthesis.)

Model 2 "Tyr10"" multiple EXAFS data fits			DFT
Samples	1, 3 and 4	5 and 6	
S_0^2	0.94 (0.04)	0.88 (0.06)	
ΔE_0			
Sample 1	-0.2 (0.4)		
Sample 3	-0.2 (0.5)		
Sample 4	0.0 (0.5)		
Sample 5		0.3 (0.7)	
Sample 6		0.4 (0.8)	
r_1 (His6)	1.98 (0.02)	1.99 (0.05)	2.05
r_2 (His13)	1.91 (0.01)	1.94 (0.05)	2.03
r_3 (His14)	2.10 (0.02)	2.06 (0.05)	2.06
r_4 (O1 from Tyr10)	1.97 (0.02)	1.94 (0.02)	2.00
r_5 (w1)	1.99 (0.02)	2.04 (0.04)	2.41
r_6 (w2)	2.32 (0.01)	2.26 (0.01)	2.78
r_7 ("solvent")	4.44 (0.02)	4.46 (0.02)	
ϕ_1 (His6)	5.2 (0.7)	0.6 (2.9)	-3.3
ϕ_2 (His13)	-1.8 (7.4)	-1.7 (12.5)	-5.3
ϕ_3 (His14)	-6.5 (0.5)	-9.6 (3.5)	-11.8
ϕ_4 (Tyr10)*	134.0 (0.0)	134.0 (2.9)	124.5
σ^2 (1st shell)	0.0027 (0.0005)	0.004 (0.001)	
σ^2 (2nd shell)†	0.0027 (0.0005)	0.004 (0.001)	
σ^2 (3rd shell)†	0.0041 (0.0006)	0.004 (0.001)	
σ^2 ("solvent")	0.007 (0.002)	0.004 (0.002)	
N_{ind}	111	72	
N_{var}	17	16	
χ^2	5.790	1.748	
R_{all}‡	0.0192	0.0335	
R_1	0.0126		
R_3	0.0231		
R_4	0.0220		
R_5		0.0310	
R_6		0.0360	

*Cu-O_h-C_ζ angle.

† Debye-Waller terms for peptide atoms at the 2nd shell (2.3Å < r < 4.0Å) and at the 3rd shell (r > 4.0Å), respectively, adjusted by the estimated coefficients A_2 and A_3: σ^2(2st shell)=A_2xσ^2 (1st shell) and σ^2(3rd shell)=A_3xσ^2 (1st shell).

‡ All R-factors are calculated in r-space and R_n factors are partial factors for multiple data sets used in refinements.

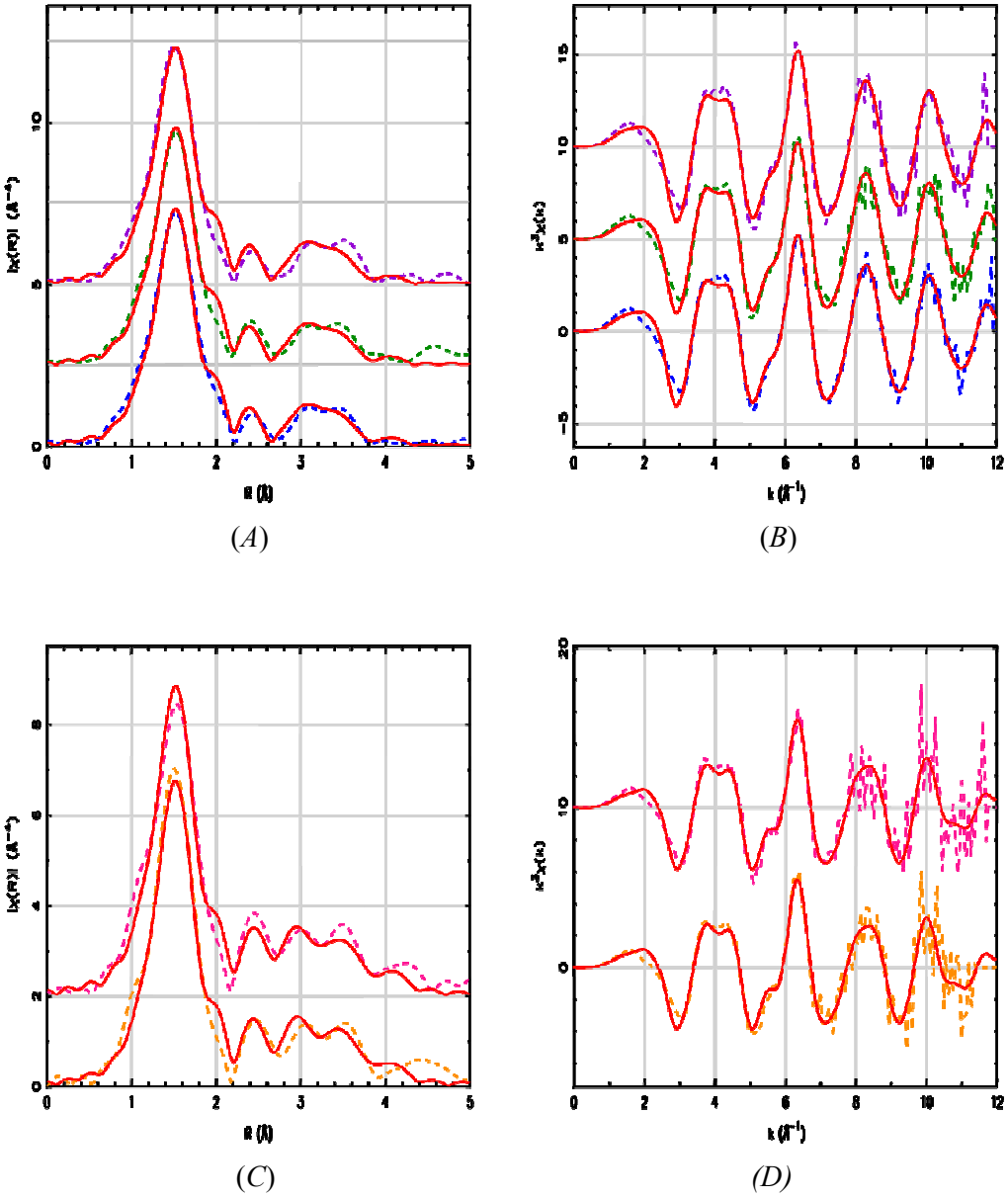

FIGURE 4S Model 2 (Tyr10) best fits of the Cu *K*-edge k^3-weighted EXAFS (*A* and *C*) and (*B* and *D*) the corresponding Fourier transforms for five Aβ-Cu^{2+} samples used in two separate multi-data refinements: (*A* and *B*) samples: 1-blue, 3-green, 4-violet and for (*C* and *D*) samples: 5-orange and 6-pink. The solid red lines are the theory; the dashed colored lines correspond to experimental data. The spectra are stacked with offset 2.5 (*A*), 2 (*B*), 2 (*C*), and 10 (*D*) units along the vertical axes.

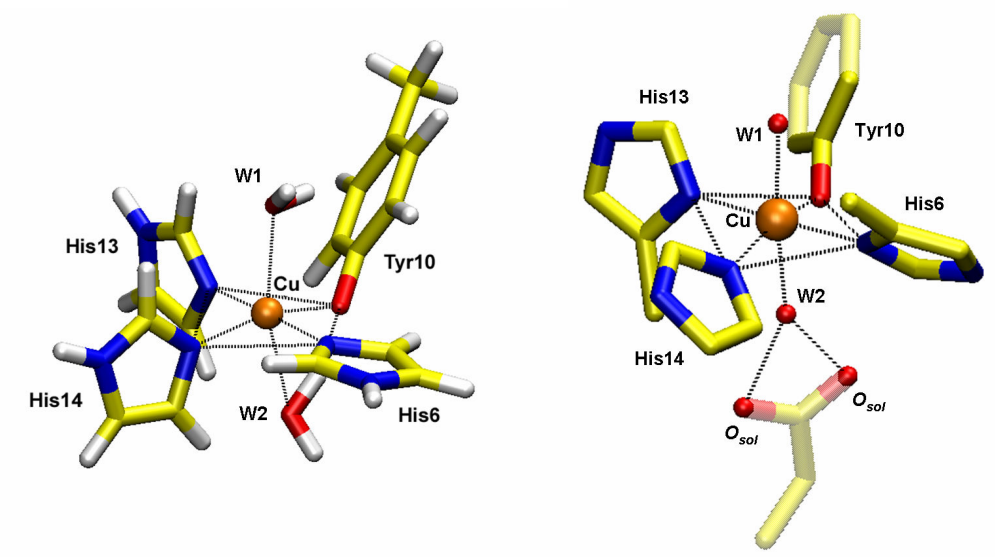

(*A*) (*B*)

FIGURE 5S A ball and stick representation of Model 2 ("Tyr10") from (*A*) DFT optimization and (*B*) EXAFS refinement of 1, 3 and 4 data sets. Axial oxygen atoms are labeled as waters W1 and W2. The two additional 'solvent" oxygen (O_{sol}) atoms (*B*) may belong to the carboxylate group from the N-terminal amino acids such as Asp1, which may participate in a hydrogen-bonding with axial water W1 to stabilize the Cu binding site. Parts of the EXAFS structure (*B*) not included in the refinement are shown in transparent colors.

REFERENCES

1. Stern, E. A. 1993. Number of relevant independent points in X-ray absorption fine-structure spectra. *Phys. Rev. B*. 48:9825-9827.
2. Newville, M. 2001. IFEFFIT: interactive XAFS analysis and FEFF fitting. *J. Synchr. Rad.* 8:322-324.
3. Draper, N. R., and H. Smith. 1998. Applied regression analysis. *New York: Wiley*:736p.
4. Michalowicz, A., K. Provost, S. Laruelle, A. Mimouni, and G. Vlaic. 1999. F-test in EXAFS fitting of structural models. *J. Synchr. Rad.* 6:233-235.
5. Klementev, K. V. 2001. Statistical evaluations in fitting problems. *J. Synchr. Rad.* 8:270-272.